

# Studies of the changes in the geometry of grain boundaries and grains during recovery/continuous recrystallization in $\alpha$ -Fe

B. RALPH

*Department of Materials Technology, Brunel, the University of West London, Uxbridge, Middlesex UB8 3PH, UK*

K. J. KURZYDŁOWSKI, A. CHOJNACKA

*Department of Material Science and Engineering, Warsaw University of Technology, 02-524 Warsaw, Narbutta 85, Poland*

Samples of  $\alpha$ -Fe (Armco) have been deformed by 50% in compression. These have then been annealed at 400 °C, considerably below the conventional recrystallization temperature, and the evolution of grain size and shape quantified. Initially the grain size is found to decrease whilst, at the same time, the grain-shape anisotropy also decreases. It is suggested that a continuous recrystallization process which favours the generation of higher angle grain boundaries is the underlying mechanism. Annealing for longer times gives rise to an increase in grain size with the development of undulations on the grain surfaces. The mechanism suggested for this behaviour involves the annihilation of segments of sub-boundaries on to a pre-existing boundary from either side of the boundary.

## 1. Introduction

Plastic deformation changes the geometry, microstructure and, as a result, properties of materials. In the case of polycrystals deformed at a low temperature, the major changes are an increase in the density of lattice defects and the rearrangement of the grain boundaries, which in the annealed state tend to form regular three-dimensional honeycomb structures [1]. These microstructural changes mean that the deformed material acquires an additional internal energy (so-called stored energy) and transforms to a new deformation-induced metastable state as the annealing progresses. The degree of microstructural change depends on the amount of deformation absorbed and the annealing temperature.

Grains in a polycrystalline aggregate strained at a low temperature tend to change their geometry in a manner similar to the overall changes in the geometry of the deformed specimen. In the case of a tensile test they gradually elongate in the direction of straining, while in a compression situation they become elongated in the directions perpendicular to the axis of straining. In both cases, profound changes are observed in the arrangement of the grain boundaries with a clear anisotropy in the grain-boundary spatial distribution which may often be related to the anisotropy of the properties of the material.

Upon annealing, the deformed microstructure tends to release stored energy and to equilibrate its microstructure. This is usually accompanied by a re-establishment of some of the properties; the phenomenon being termed static recovery. The term "static" underlines that recovery does not act concurrently with the

deformation process, which it does in the "warm" range where dynamic recovery occurs.

It is commonly known that the recovery is characterized by a decrease in the density of point defects (vacancies and self interstitial atoms) and a rearrangement of dislocations which reform into more stable configurations in the form of dislocation walls [2]. However, in the case of polycrystals, an important role may also be played by processes taking place at grain boundaries. Grain boundaries are a major strengthening factor of the microstructure of polycrystals and their non-equilibrium geometry and arrangement as a result of plastic deformation contributes to work hardening of the material. Upon annealing of deformed polycrystals, the rearranged grain boundaries are expected to migrate to more equilibrium positions, accelerating this annihilation of the dislocations.

A possible role for grain boundaries in the process of recovery has been suggested elsewhere [3, 4]. However, in these previous studies, materials were only lightly deformed, to less than 5% tensile strain, and the total effect was relatively small. The present communication reports studies of the same phenomenon in a material subjected to significantly larger levels of deformation. It was also decided to use  $\alpha$ -Fe instead of the  $\gamma$ -Fe and nickel used in the previous studies, in order to make any possible conclusions more general.

## 2. Experimental procedure

The studies were performed on  $\alpha$ -Fe (Armco) with an initial grain size of approximately 60  $\mu\text{m}$ . The chemical composition of the material is given in Table I.

TABLE I The chemical composition of the material used ( $\alpha$ -Fe Armco B, symbol: E04A) in weight percentages.

| C      | Mn     | Si     | P       | S       | Fe      |
|--------|--------|--------|---------|---------|---------|
| < 0.04 | < 0.10 | < 0.01 | < 0.020 | < 0.025 | balance |

TABLE II Times of annealing of 400 °C and the resulting variation in hardness, means values,  $E$ , of equivalent diameter,  $d_{eq}$ , calculated intercept length,  $l$ , and the ratios defining the shape of grains (see the text). Coefficients of variation of the equivalent diameter distribution are also given.

| Time (h) | Hardness (HB) | $E(d_{eq})$ ( $\mu\text{m}$ ) | $CV(d_{eq})$ | $E(l)$ ( $\mu\text{m}$ ) | $E(d_{max}/d_{eq})$ | $E(p/p_c)$ |
|----------|---------------|-------------------------------|--------------|--------------------------|---------------------|------------|
| 0        | 161           | 60.3                          | 0.65         | 51.2                     | 1.58                | 1.14       |
| 0.5      | 147           | 50.3                          | 0.67         | 47.9                     | 1.33                | 1.17       |
| 1        | 146           | 57.7                          | 0.63         | 50.4                     | 1.37                | 1.22       |
| 3        | 143           | 61.4                          | 0.71         | 59.3                     | 1.38                | 1.25       |
| 8        | 134           | 66.0                          | 0.79         | 66.9                     | 1.32                | 1.46       |

TABLE III Temperatures for 1 h anneals and the resulting variation in hardness, means values ( $E$ ) of equivalent diameter  $d_{eq}$ , and the ratios defining the shape of grains (see the text). The coefficient of variation of the equivalent diameter distribution is also given

| Temp. (°C) | Hardness (%) | $E(d_{eq})$ ( $\mu\text{m}$ ) | $CV(d_{eq})$ | $E(d_{max}/d_{eq})$ | $E(p/p_c)$ |
|------------|--------------|-------------------------------|--------------|---------------------|------------|
| RT         | 100          | 60.3                          | 0.65         | 1.58                | 1.14       |
| 600        | 71           | 21.9                          | 0.69         | 1.31                | 1.17       |
| 700        | 62           | 26.5                          | 0.62         | 1.30                | 1.12       |
| 800        | 61           | 35.6                          | 0.64         | 1.30                | 1.16       |

Specimens in the form of rods were compressed at room temperature to give a total reduction in thickness of 50%. The deformed material was isothermally annealed at 400 °C for the annealing times given in Table II. In order to establish a reference level for the properties of the material, some specimens were also annealed in the range 600–800 °C and for 1–3 h. These specimens were found to be fully recrystallized with a grain size significantly smaller than the initial one. The results for 1 h anneals are given in Table III.

The specimens used for the quantitative characterization of the microstructures were prepared by vertical sectioning. This method assumes that the observation planes are parallel to a specified direction and in our case they were parallel to the direction of deformation (see Fig. 1). Specimens were mechanically polished and electrolytically etched to reveal the grain-boundary networks according to standard metallographic procedures.

In the observations of the microstructure in the specimens annealed under different conditions, attention was focused on the description of the overall grain-boundary geometry. This geometry has been described through measurements of grain-boundary traces revealed on the cross-sections of the specimens. The following parameters have been used:  $S_v$ , grain-boundary area per unit volume;  $A_i$ , area of an individual grain section;  $d_{eq}$ , equivalent diameter of grain

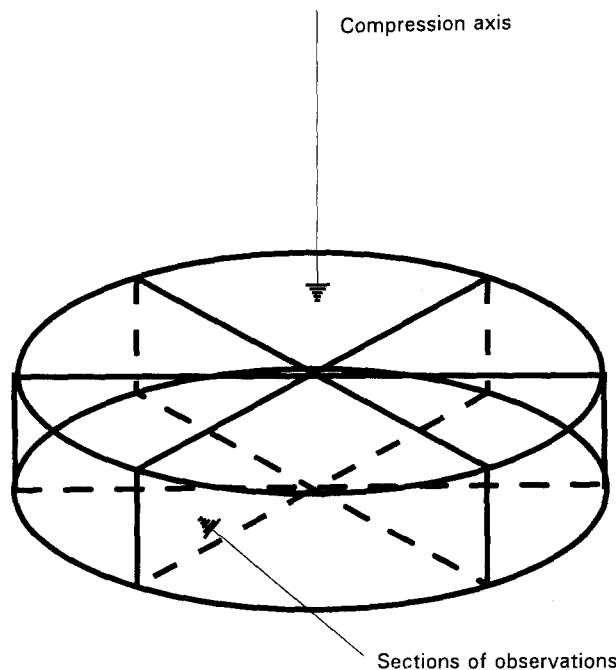


Figure 1 Schematic drawing of the geometry of the specimens and the section planes.

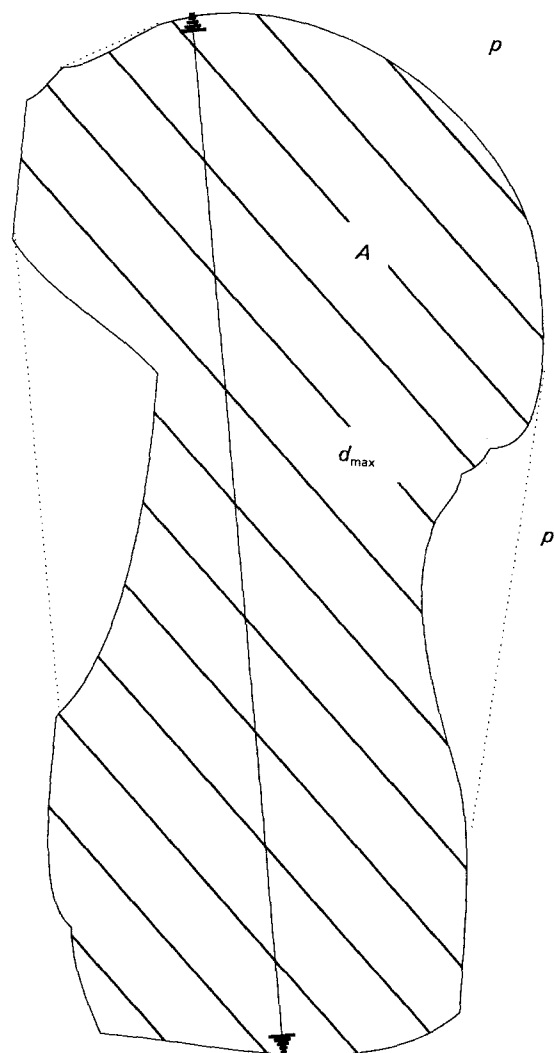


Figure 2 Definition of the parameters used to describe geometry of the grains and grain boundaries revealed on the sections of the material.

sections computed as the diameter of the same are a circle;  $d_{\max}$ , maximum chord of the grain section;  $p$ , grain section perimeter;  $p_c$ , grain section Cauchy perimeter. A geometrical interpretation of these parameters is given in Fig. 2. Among the parameters used,  $S_v$  defines the density of the grain boundaries, while  $A_i$  and  $d_{eq}$  are measures of the size of grains. Some of these parameters are particularly sensitive to microscopic resolution, so this has been standardized. Because measurements were carried out for individual grains, these parameters provided information on the mean size,  $E(A)$  and  $E(d_{eq})$ , (the symbol  $E(x)$  is used in the text to indicate the mean value of variable  $x$ ), and on the spread in the size of grains in terms of the coefficient of variation  $CV(A)$  and  $CV(d_{eq})$ . ( $CV(x) = SD(x)/E(x)$  where  $SD(x)$  is the standard deviation of  $x$ ). The last two parameters listed have been used to define two shape factors: (a)  $d_{\max}/d_{eq}$  and (b)  $p/p_c$ .

The first shape factor is a sensitive measure of grain elongation. It is equal to 1.0 for a circle and in the range 1.30–1.35 for as-annealed  $\alpha$ -Fe. The second ratio can be used to measure the degree of non-convexity of grain sections. It is equal to 1.0 for convex figures and is in the range from 1.1–1.2 for the annealed microstructures.

The measurement of these geometrical parameters was made with the help of an automatic image analysis system. The measurements of  $S_v$ , due to the anisotropy of the microstructure, were carried out using the procedure based on vertical sectioning and employing cycloids (see, for example, [5]). The values of  $S_v$  have been used subsequently to determine true mean random intercept length  $E(I)$  from the relationship

$$S_v = \frac{2}{E(I)} \quad (1)$$

It should be remembered that this parameter cannot be obtained from a simple test with a grid of lines due to the anisotropy in the system of the grain-boundary traces. All measurements were made on the images at the same magnification to avoid complications of using fractal analysis of the perimeter length.

In addition to the measurements of the geometry of grains and grain boundaries, the hardness of the samples was measured.

### 3. Results

Fig. 3 shows micrographs characteristic of the microstructure of the material after 50% compression and the subsequent anneals. It can be noted that the sections of the grains in the deformed material are clearly elongated in the direction perpendicular to the axis of straining. The microstructures revealed on sections of specimens after annealing at 400 °C (for 0.5, 1, 3 and 8 h) show successive stages of grain-boundary rearrangement in the process of continuous recrystallization. After 30 min annealing, the grain boundaries have lost their preferential orientation along the direction perpendicular to the axis of straining. The shape factor  $d_{\max}/d_{eq}$ , plotted against the time of annealing in Fig. 4, shows a drop in value from 1.6 to 1.3, the

latter value being typical of annealed  $\alpha$ -Fe. This value remains effectively unchanged with longer annealing times. At the same time, the grain boundaries revealed in cross-sections become more curved and lose their predominantly convex shape. These changes are reflected by increasing values of  $p/p_c$  (see Fig. 4).

Annealing of the deformed material at 400 °C also results in a change in the total grain-boundary area as shown in Fig. 5. The grain-boundary area per unit volume,  $S_v$ , in the beginning increases in value by approximately 5% and then gradually drops by 20% after an 8 h anneal. As a result, the mean intercept length decreases in the first stage of the recovery and then steadily increases as recovery/continuous recrystallization proceeds. The observed rearrangement of the grain boundaries is accompanied by a systematic increase in the spread in grain-size distribution, as indicated by increasing values of  $CV(A)$  and  $CV(d_{eq})$  depicted in Fig. 6.

The observed changes in the geometry of the grain-boundary array correlate well with the variation in the hardness of the material. There is a sharp initial drop in the hardness after 30 min annealing at 400 °C followed by a slower decrease for longer annealing times (see Fig. 7).

### 4. Discussion

When samples of this material are annealed at temperatures from 600–800 °C, conventional, discontinuous recrystallization occurs, giving a completely new set of grains by a mechanism involving nucleation and growth. However, the annealing schedules at 400 °C (which is below the conventional recrystallization temperature) still alter the grain-boundary geometry. The present investigation shows that grain boundaries undergo profound changes in their geometry in the processes of recovery/continuous recrystallization.

There are some characteristic stages in the variation of the grain-boundary geometry as a function of annealing time at 400 °C. Initially, for times of annealing in the range of 30 min, the boundaries restore their near-equilibrium geometry by decreasing their elongation. This is accompanied by an increase in the total density of the grain boundaries (i.e. a reduced grain size) and a rapid decrease in hardness. Both of these features suggest that this rearrangement is partly due to a rapid sub-grain growth which gives larger sub-grains with relatively higher angle sub-boundaries of misorientation angle exceeding 10° [2, 6]. As a result of the etching, these sub-boundaries are revealed in the micrographs as elements of the grain-boundary network. The network of higher angle sub-boundaries, revealed by etching, gives rise to an overall grain-boundary geometry which is more isotropic and regular in terms of the grain shape. This means that the sub-boundaries which undergo an accelerated accumulation of misorientation are oriented at approximately right angles to the direction of elongation. This must mean that the pattern of the deformation, which is itself anisotropic drives the preferential creation of the grain pattern observed.

In the second stage, the grain boundaries gradually

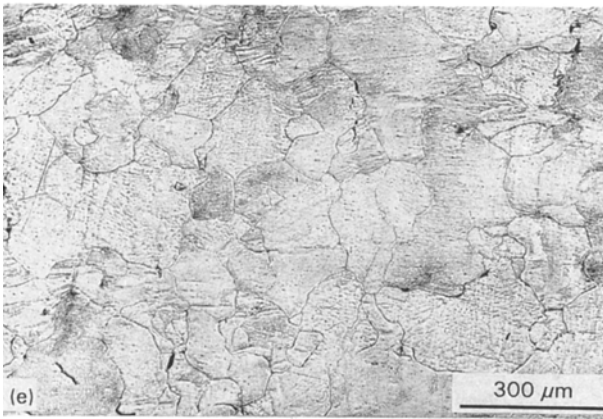
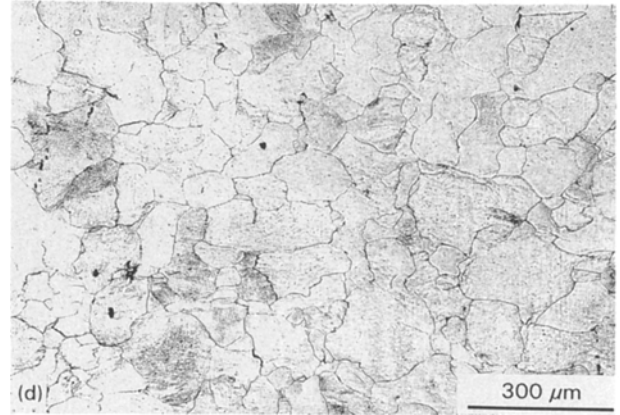
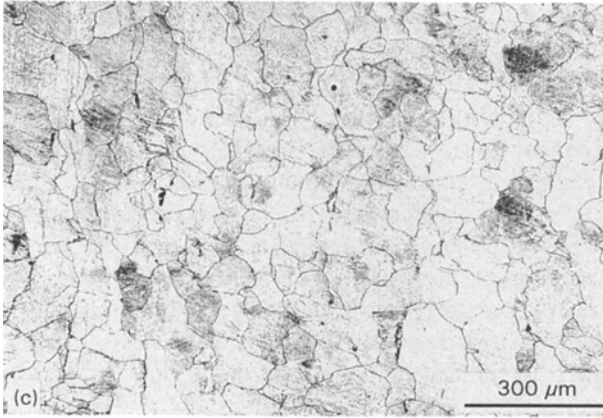
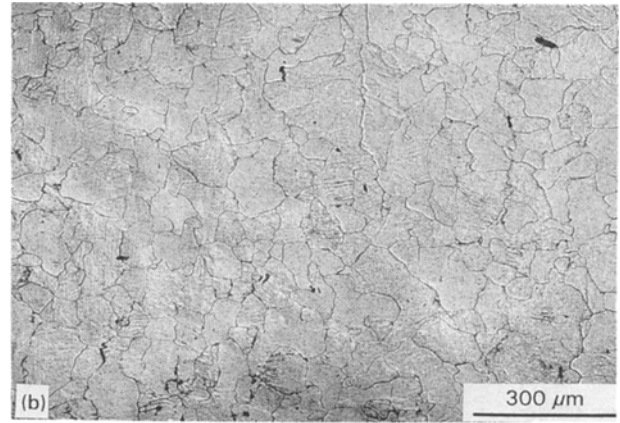
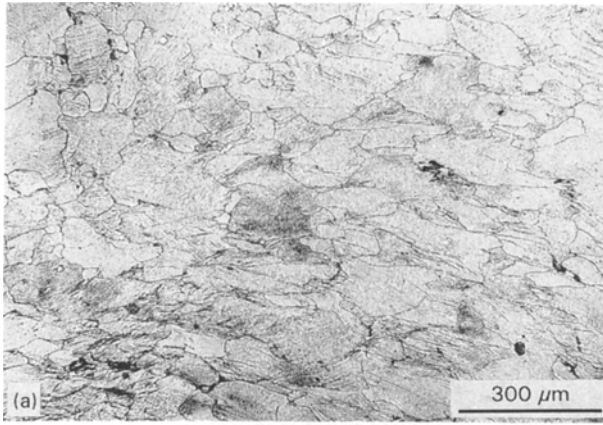


Figure 3 Micrographs characteristic of the microstructures of the material after (a) compression, (b) subsequent annealing at 400°C for 30 min; (c–e) subsequent annealing at 400°C for 1, 3 and 8 h, respectively.

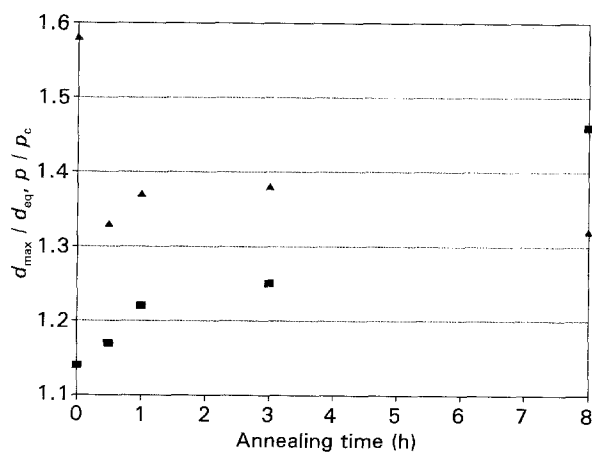


Figure 4 Plot of shape factors, means values of (▲)  $d_{\max}/d_{\text{eq}}$  and (■)  $p/p_c$ , against the annealing time at 400°C.

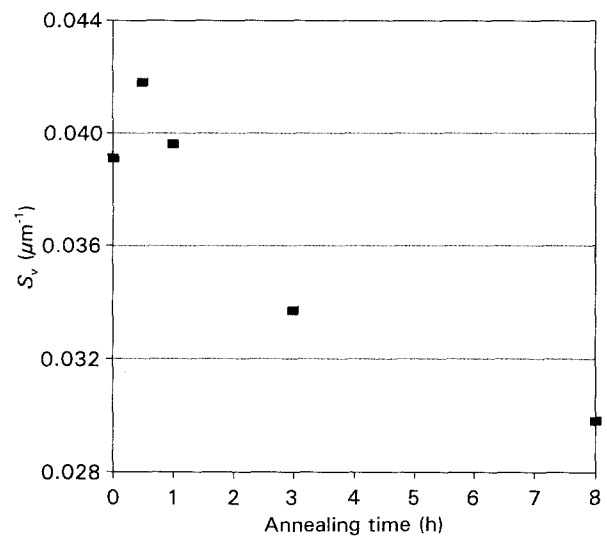


Figure 5 Variation in the density of the grain boundaries,  $S_v$ , as a function of annealing time at 400°C.

reduce their surface area leading to a grain size increase. At the same time they develop a more overall concave shape with a clear tendency for local undulations. As these two tendencies are in contradiction (convex figures have smaller surface areas) it can be concluded that the changes in the grain-boundary rearrangement are driven by the reduction of their

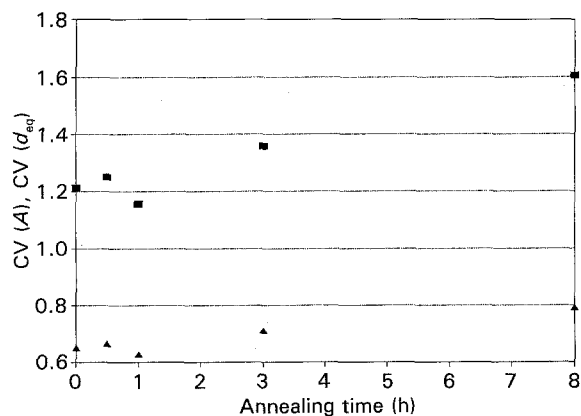


Figure 6 Variation in (■) CV (A) and (▲) CV ( $d_{eq}$ ) as a function of annealing time at 400°C.

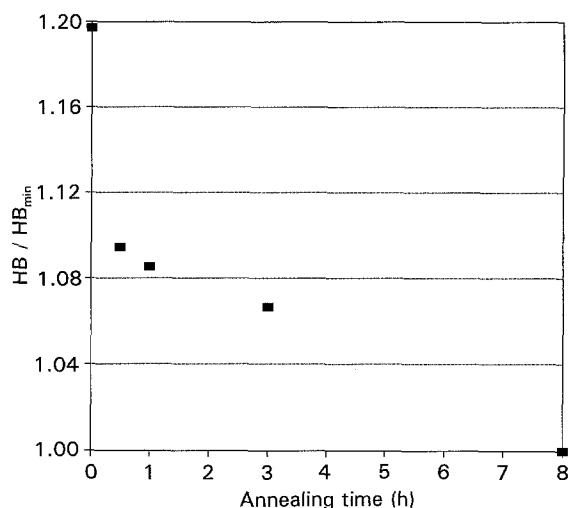


Figure 7 Variations in the hardness normalized to the hardness after 8 h annealing at 400°C.

surface area, on the one hand, and by the annihilation on them of segments of the sub-grain boundaries, on the other. This is accompanied by an increasing width in the grain-size distribution which is an indication of a drift towards abnormal grain growth, a phenomenon frequently observed in strained materials. It is believed that the undulations seen on the pre-existing grain boundaries reflect a tendency for sub-boundaries on either side of them to annihilate in segments from either side. In essence, this proposal incorporates the ideas of strain-induced grain-boundary migration [7, 8] and nucleation of recrystallization by accelerated sub-grain coalescence [9] previously offered. In addition, the geometrical means by which a more equiaxed pattern of grain boundaries is generated agrees well with the proposals of Gudmundsson *et al.* [10].

The two stages of the grain-boundary rearrangement correlate with two stages in the recovery of the hardness. An initial increase in the total area of the

grain boundaries is accompanied by a rapid drop in the hardness. A more gradual increase in the grain-boundary undulations, accompanied by an increase in grain size and a widening of the grain-size distribution function is combined with a slower decrease in the hardness.

These observations suggest that grain boundaries play a role in the changes accompanying recovery and continuous recrystallization. In the present study, coarse-grained polycrystals were used in order to make it easier to quantify the grain geometry. However, the effect of the arrangement of the grain boundaries on the properties of materials can be inferred and is expected to be even more significant for fine-grained polycrystals. Further studies of the phenomenon, using techniques at higher resolutions, are in progress.

## 5. Conclusion

The processes which occur when deformed polycrystals are annealed are complex. It is usual to term the processes occurring below the recrystallization temperature under the overall title of, recovery, where the grain pattern is largely unchanged. However, the study reported here shows that grain boundaries can play an important part in annealing processes below the recrystallization temperature and this can lead to major alterations in the grain-boundary pattern.

## Acknowledgement

The authors are grateful to the EC PECO programme for supporting the visit of K.J.K. to Brunel University.

## References

1. F. N. RHINES, "Microstructology, Behavior and Microstructure of Materials" (Rieder Stuttgart, 1986).
2. B. RALPH, C. BARLOW, B. COOKE and A. PORTER, in "1st Risø International Symposium on Metallurgy and Materials Science", edited by N. Hansen, A. R. Jones and T. Leffers (Risø press, Roskilde, Denmark, 1980) p. 229.
3. K. J. KURZYDŁOWSKI, S. SANGAL and K. TANGRI *Metall. Trans.* **20A** (1989) 471.
4. K. J. KURZYDŁOWSKI, *Scripta Metall. Mater.* **27** (1992) 871.
5. A. J. BADDELEY, H. J. G. GUNDERSEN and L.-M. CRUZ-ORIVE, *J. Microsc.* **142** (1986) 259.
6. A. R. JONES, P. R. HOWELL and B. RALPH, *Philos. Mag.* **35** (1975) 603.
7. P. A. BECK and P. R. SPERRY, *J. Appl. Phys.* **21** (1950) 150.
8. J. E. BAILEY and P. B. HIRSCH, *Proc. Roy. Soc.* **A267** (1962) 11.
9. A. R. JONES, B. RALPH and N. HANSEN, *ibid.* **A368** (1979) 345.
10. H. GUDMUNDSSON, D. BROOKS and J. A. WERT *Acta Metall. Mater.* **39** (1991) 19.

Received 30 September  
and accepted 1 November 1993